Bulletin of the Seismological Society of America, Vol. 92, No. 4, pp. 1570–1576, May 2002

High-Resolution Topography along Surface Rupture of the 16 October 1999 Hector Mine, California, Earthquake (M_w 7.1) from Airborne Laser Swath Mapping

by K. W. Hudnut, A. Borsa, C. Glennie, and J.-B. Minster

Abstract In order to document surface rupture associated with the Hector Mine earthquake, in particular, the area of maximum slip and the deformed surface of Lavic Lake playa, we acquired high-resolution data using relatively new topographic-mapping methods. We performed a raster-laser scan of the main surface breaks along the entire rupture zone, as well as along an unruptured portion of the Bullion fault. The image of the ground surface produced by this method is highly detailed, comparable to that obtained when geologists make particularly detailed site maps for geomorphic or paleoseismic studies. In this case, however, for the first time after a surface-rupturing earthquake, the detailed mapping is along the entire fault zone rather than being confined to selected sites. These data are geodetically referenced, using the Global Positioning System, thus enabling more accurate mapping of the rupture traces. In addition, digital photographs taken along the same flight lines can be overlaid onto the precise topographic data, improving terrain visualization. We demonstrate the potential of these techniques for measuring fault-slip vectors.

Introduction

The 16 October 1999 Hector Mine, California, earthquake (M_w 7.1) was associated with extensive surface rupture (Fig. 1). Across Lavic Lake playa, for example, slip in the range of 2.0–3.0 m displaced the formerly quasi-planar playa surface into remarkable geomorphic expressions of compressional and dilational jogs and steps. As with all surface-rupturing earthquakes, it was considered imperative to document the rupture quickly and in great detail to better understand the faulting process. Two days after the earthquake, I. K. Curtis, on contract for the U.S. Geological Survey (USGS) and at the earliest opportunity allowed by the U. S. Marine Corps (USMC), acquired aerial photographs at a scale of 1:10,000 and 1:3,000. Subsequent geologic mapping has employed these air photos, as well as pre-earthquake imagery provided by the USMC (and various USGS and USMC topographic maps of the area). With these resources available, geologists recorded the surface ruptures in detail (e.g., USGS, SCEC, and CDMG Scientists, 2000; Treiman *et al.*, 2002). Treiman *et al.* (2002) reported 48 km of surface breaks that offset geomorphic features by as much as 5.25 m. Furthermore, Interferometric Synthetic Aperture Radar (InSAR) enabled the mapping of surface ruptures that in some cases, had eluded field geologists (e.g., Sandwell *et al.*, 2001; Simons *et al.*, 2002). Documentation of surficial ruptures of this earthquake, then, relied on the strengths of established methods while also benefiting from novel approaches and the extensive use of both airborne and satellite remote-sensing data. Limited access on the USMC base made documenting the surface rupture by standard field methods more challenging, so the acquisition of remote-sensing data and development of new methods to study this earthquake turned out to be both timely and fortuitous.

In studies of fault-zone geomorphic features, geologists often employ high-precision mapping methods in order to document features offset by surface ruptures. It is desirable to quantify surface deformation at a level of precision that captures the complexity of faulting and the details of surficial features that are offset by the faulting. Precise methods have recently been developed for field mapping, including electro-optical "total station" and real-time kinematic Global Positioning System (GPS) techniques. For example, in their study of the 1987 Superstition Hills earthquake, Lindvall *et al.* (1989) made highly detailed topographic maps of offset features that had contour intervals as fine as 2 cm. In addition, Kurushin *et al.* (1997) extensively documented offset features along the surface-rupture traces of the 4 December 1957 Gobi-Altay, Mongolia, earthquake. In that case, field parties made detailed topographic maps, profiles, and pho-

Any use of trade, product, or company names in this report is for descriptive purposes only and does not necessarily imply endorsement by the U.S. Government.

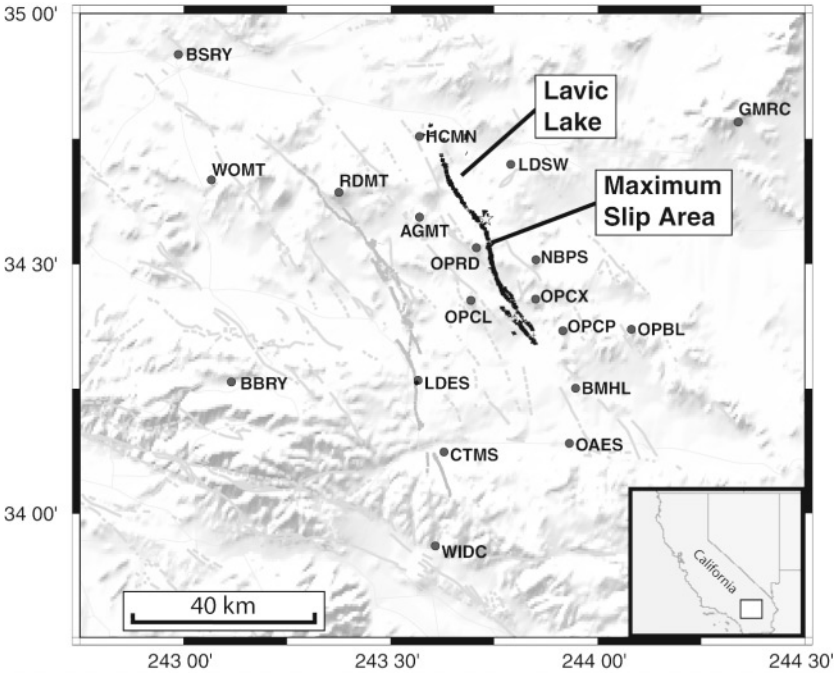

Figure 1. Map showing the location of the 1999 Hector Mine earthquake surface rupture (from Treiman *et al.*, 2002) and stations of the SCIGN that were used for positioning of the aircraft platforms used in obtaining the laser-scanning and digital imagery for this study (from Hudnut *et al.*, 2002). The locations shown in Figures 2, 4, 5, and 6 are all within the indicated maximum-slip area, whereas Figure 3 shows views of Lavic Lake playa. The Hector Mine earthquake epicenter is indicated by a star, and faults and highways are shown as gray lines.

tographs of 46 sites along the surface rupture to provide accurate information for this great earthquake. In general, it is desirable that such documentation be made as comprehensive and objective as possible.

As with previous studies, testing the ideas of characteristic slip events and segmentation also motivated the present study. We wished to further improve the quantification of surface ruptures for this and future earthquakes. With the data obtained in our study, it should be possible to extend the capabilities for modeling of surface processes and to use quantitative geomorphological methods to understand the history of prior earthquakes on this fault system. Also, it should be possible to model the effects on topography of repeated slip events with either similar or differing slip distributions, in order to evaluate whether or not crucial faulting parameters, such as the slip distribution per event and end points of rupture, are constant (in either space or time).

Methods

We scanned the maximum-slip area and the deformed surface of Lavic Lake playa (Fig. 1), as well as the remainder of the main surface rupture and an unruptured portion of the Bullion fault by using a raster-laser approach. Airborne Laser Swath Mapping (ALSM), also known as light detection and ranging, or simply laser scanning, is becoming an increasingly precise and commercially available topographic-mapping method (e.g., Krabill *et al.*, 1995; Carter and Shrestha, 1997; Ridgeway *et al.*, 1997; Burnman, 2000). Ground control was supplied by remotely setting several of the recently installed Southern California Integrated GPS Network (SCIGN) continuously operating GPS stations (Hudnut *et al.*, 2002) to record at sampling rates of up to 2 Hz during the data-acquisition flights.

On 19 April 2000, a field team acquired the entire data set using a "TopEye" laser-scan device manufactured by Saab Survey Systems. The laser scanner was flown aboard a Eurocopter AS 350 BA helicopter, so as to provide a stable and maneuverable airborne platform. Onboard GPS and an integrated inertial-navigation system allowed precise positioning of the platform and its scanning-system optics during data acquisition. The instrument system is composed of an integrated, inertially stabilized platform, dual-frequency GPS positioning, and an accurate pulsing-and-scanning laser range-finding system. The laser scanned at a rate of 6,888 outgoing pulses per second, and the system then detected the reflected laser light and the round-trip travel time of each pulse, which was used to measure the distance from the laser to the ground. The system recorded delays and intensities of up to four return pulses per outgoing pulse. Onboard computers collected, correlated, and recorded the laser scan and the airborne GPS data for postprocessing. A navigation system on the helicopter controlled the flight path, such that the pilot would not need to rely on ground-based landmarks.

Precise way-point navigation was defined on the basis of the coordinates of slip-measurement site localities and fault-segment end points that were identified in the field (Treiman *et al.*, 2002). A swath width of $\sim$125 m on average, along $>$70 km of flight lines, was obtained in a single day, covering all of the main fault breaks known at that time (Fig. 1). Along the maximum-slip area and at Lavic Lake, a swath width of 200 m was obtained in overlapping, multiple data passes. In addition, a fault-perpendicular swath was run across Lavic Lake to attempt to detect longer-wavelength deformation of the dry lake bed.

We performed calibration maneuvers to assess instrumentation and software unknowns and error sources. We also collected redundant data over the Hector Mine open-pit-excavation area that had previously been mapped in detail using conventional photogrammetric methods. These data will enable comparisons with other methods and assessments of the geodetic capabilities attainable by repeat passes made at different times.

The ALSM system yielded data files from the proprietary laser-scanning package that contained the following quantities for each sample: (1) time; (2) aircraft position in World Geodetic System 1984 (WGS84) latitude, longitude, and ellipsoidal elevation; (3) aircraft attitude; (4) raw laser range; (5) pitch and angle mirror adjustments; (6) laser nadir angle; (7) vertical component of laser range; and (8) the WGS84 Cartesian coordinates of the laser target. An example of a "point cloud", showing the raw laser-ranging data, is shown in Figure 2. In places along the fault, hundreds of laser "hits" were collected per square meter of ground surface. The faulted ground surface was imaged with resolution sufficient to identify the surface breaks by manipulation and close visual inspection of the raw laser-scanning data in three dimensions. The data can then be displayed as artificially illuminated surfaces, as in Figure 3a.

These ALSM data allowed systematic production of a high-resolution topographic map with 1-ft. (304.8 = mm) contour intervals on a universal transverse Mercator grid along the primary surface ruptures (these units and coordinate systems are the standard ones used for commercial products). A digital camera was flown separately aboard a fixed-wing Partenavia P68 aircraft. Each image had GPS time and position recorded for precise geolocation, and a map of air-photo centers was thereby made for indexing and geolocating the individual photographs. An example image is shown (Fig. 3b), along with a corresponding oblique-surface image (Fig. 3c) and a photograph that shows the deformed Lavic Lake playa (Fig. 3d). In addition to these individual digital photographs, a georeferenced and orthorectified, high-resolution image mosaic along the region of maximum slip on the fault was produced.

We recovered and archived all possible raw data and intermediary data from the GPS ground-control stations and the aircraft-mounted GPS instruments during all flights, as well as all of the digital images and all of the laser-scan data files. All of these data form an openly distributed data set, available at http://rincon.gps.caltech.edu/. In addition, analog videos collected using cameras mounted on the aircraft during laser-data acquisition have been archived (but are not included in the digital data set on the Internet). These videotapes are available for review at the USGS office in Pasadena, California.

Results

In Figures 4, 5, and 6, a relatively simple section of the surface rupture, ~300 m in length, is shown. The ground surface in this section slopes generally toward the northeast, and several small-scale topographic features nearly perpendicular to the fault clearly show disruption from this earthquake. Here, a roughly planar main break and relatively narrow fault zone allow a straightforward measurement of slip across the fault. Our approach was to estimate a single slip

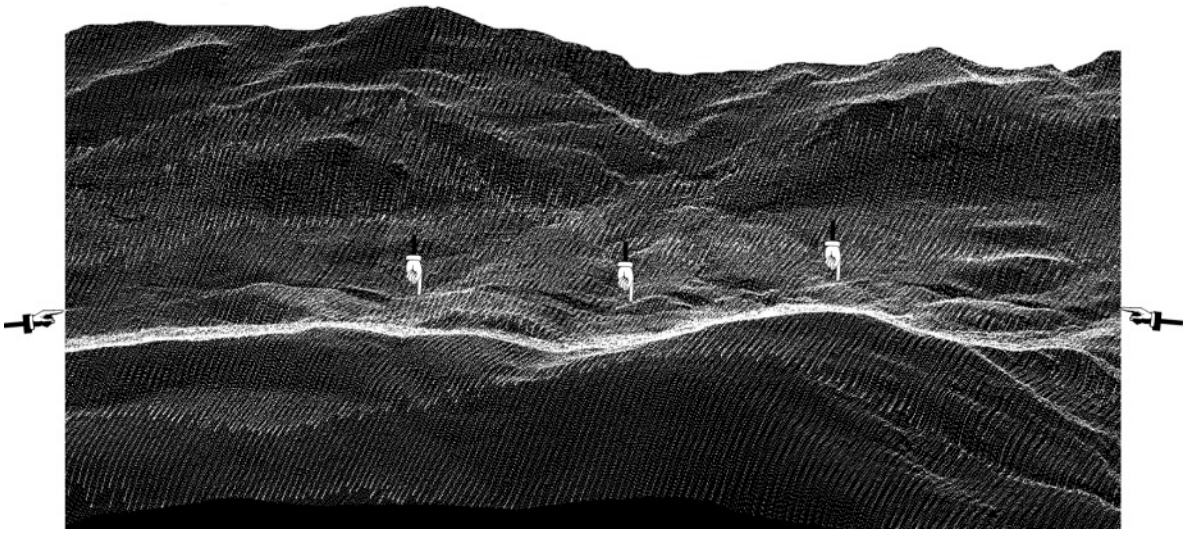

Figure 2. Oblique view of Hector Mine earthquake surface rupture that experienced 3.5–4.5 m of right-lateral displacement. The rupture trace is pointed out by finger icons; the light and dark bands below and above the surface rupture are subparallel, topographic escarpments. Several offset ridges are now juxtaposed with gullies, forming 'shutter' ridges. Raw laser hits are used to illuminate the ground surface in this point-cloud image. From tens to hundreds of hits per square meter were collected along the primary surface ruptures.

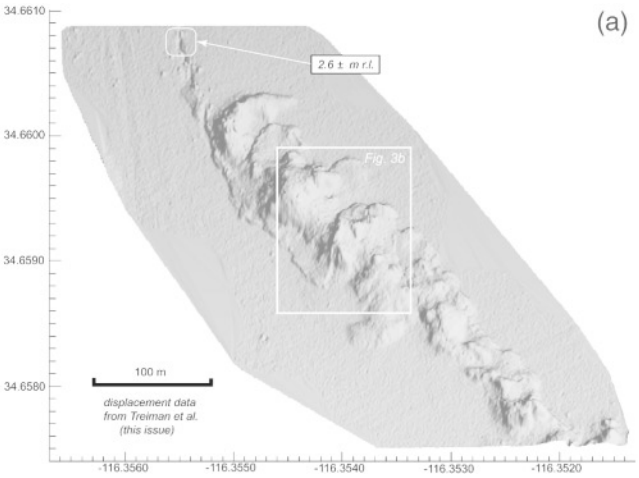

Figure 3. (a) Laser-scan data of a portion of the Lavic Lake playa, artificially illuminated from a low point in the southeast and tilted away from the viewer. The topographic feature protruding from the playa surface existed before the Hector Mine earthquake, yet these exposed lavas were thrusted upwards farther during this earthquake. This area is shown in and displacement data are from Figs. 2b and 6 of Treiman *et al.* (2002). (b) Digital aerial-photographic image for the same area of Figure 3a, showing the playa surface (gray), the lava surface (black), and the fractures and shattering (white) associated with the Hector Mine earthquake. Computer manipulation allowed enhancement of the surface-rupture pattern recorded in this image. Detailed geologic mapping has been performed for this area (Rymer *et al.*, 2002; Treiman *et al.*, 2002). The arrow indicates the location and direction from which Figure 3d was taken. (c) Oblique-surface image of laser-scan data for the same area shown in Figure 3a and 3b with an inset box indicating the location of Figure 3d. (d) Photograph of the ground surface corresponding to the view indicated by the arrow in Figure 3b, showing compressional features on the shattered surface of the Lavic Lake playa.

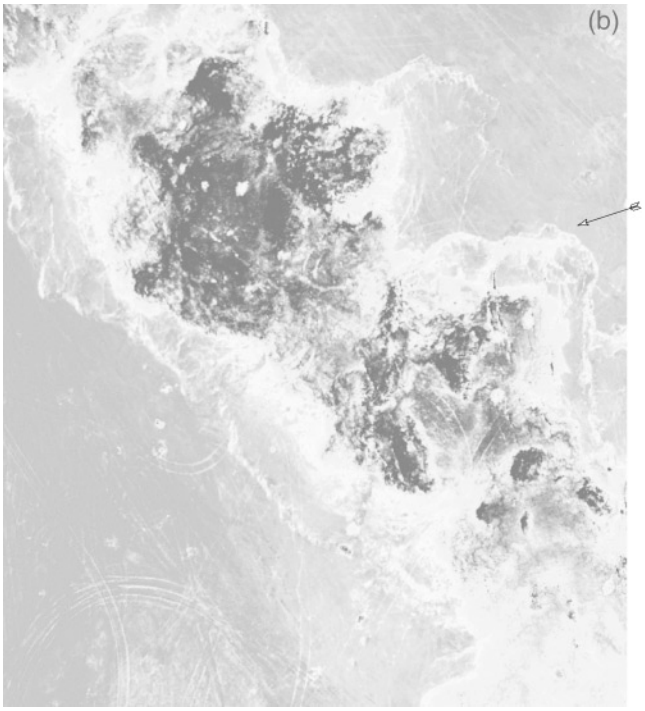

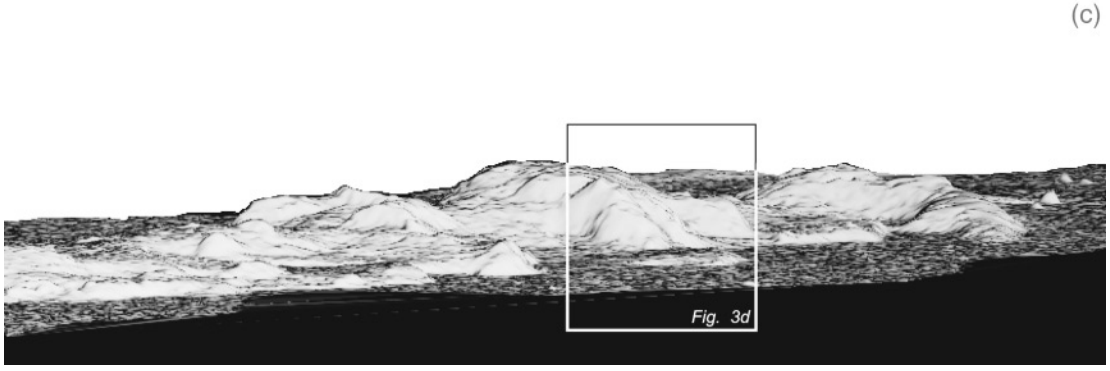

vector representing the average displacement along this part of the fault. The lines parallel to the fault trace in Figure 4 mark the locations of data used to make the cross-sectional profiles displayed in Figure 6. Analyzing these raw laser data, we have estimated the slip vector along this portion of the fault using a method devised by Borsa *et al.* (2001).

First, data taken from the two cross-section lines indicated on Figure 4 were projected onto the fault plane to correct for ground slope on either side of the fault. Neither the ground surface nor the fault is planar, of course, although we assume them to be so. These straight, profile lines each lie at a perpendicular distance from the fault, which varies from ~2–4 m on either side (because the fault itself is not exactly straight). This projection was made perpendicular to the fault plane, so topographic features that are not exactly perpendicular to the fault limit its accuracy. These projected profiles are shown in Figure 6a. Inverting for the slip vector that yielded the maximum cross correlation between the profiles, we estimated 4.2 ± 0.5 m of right-lateral slip and 0.9 ± 0.1 m of vertical slip. In Figure 6b, this displacement-vector offset was removed from the projected profiles in Figure 6a to show the quality of the match between topographic profiles on either side of the fault zone. Close comparison of the individual peaks and troughs on this set of curves shows that slip varies only slightly within this 300-m-long reach of the fault zone, with some of the apparent slip variation resulting from the limitations of the fault-plane projection.

Within the section of the fault shown in Figure 4, geologists measured right-lateral slip ranging from 3.5 to 5.1 m and variable amounts of east-side-up vertical slip ranging up to 0.3 m (Treiman *et al.*, 2002). Our measurement, therefore, seems to be in general agreement with both the horizontal and vertical components of slip measured in the field along the same fault segment. Further geological data for this section of the fault will be available for more detailed comparisons in the future (Hector Mine Geologic Working Group, 2002). Our initial result at this one site is evidently also in general agreement with the InSAR results, which show similar amounts of both vertical and horizontal slip along this section of the fault (e.g., Simons *et al.*, 2002). This example demonstrates that the ALSM method, using a single, postearthquake data acquisition, can be used to extract the relative displacement vector from near-fault topographic features.

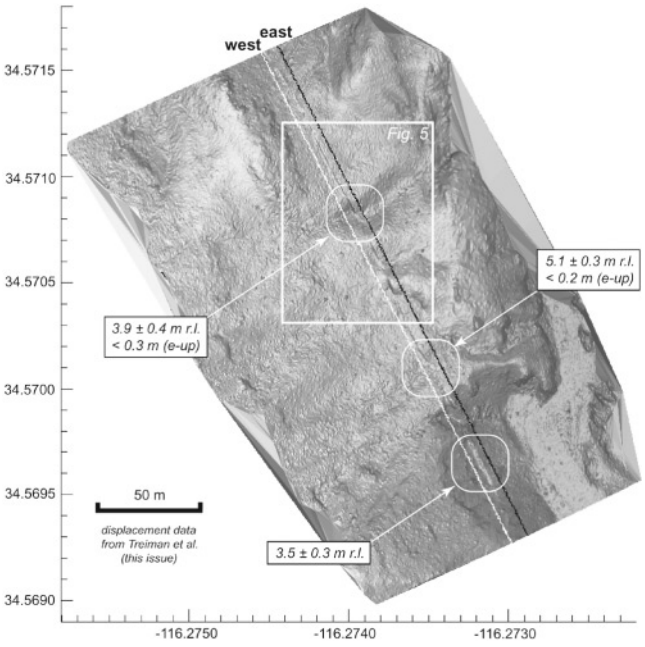

Figure 4. Shaded-relief image for the same part of the fault shown in Figures 5 and 6. Along this maximum-slip section of the surface rupture (in the Bullion Mountains), topographic features at the few-decimeter to few-meter scale are clearly offset by the surface rupture. White and black lines running parallel to the main surface break indicate the cross-sectional profiles (east and west, respectively) that are shown in Figure 6. Displacement data shown for three offset features are from Treiman *et al.* (2002).

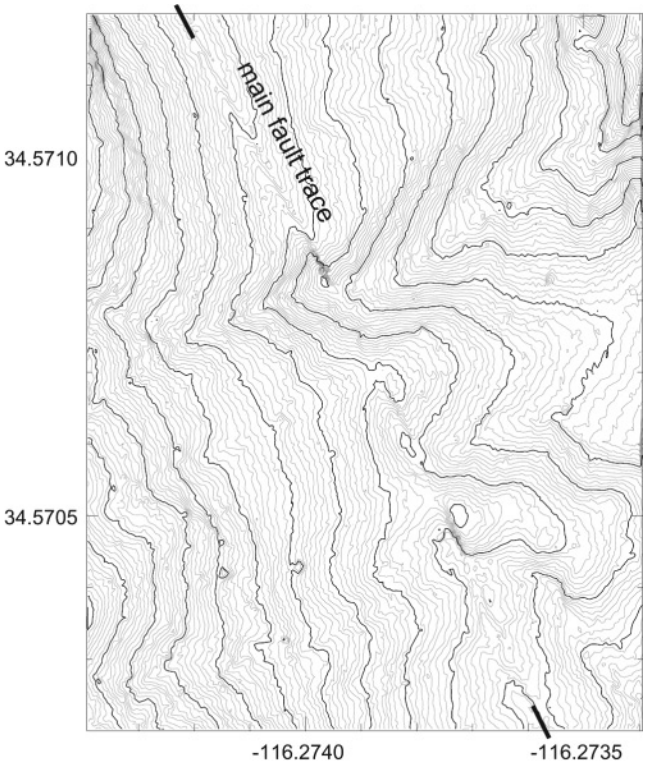

Figure 5. Topographic-contour map of the Hector Mine earthquake surface rupture along a portion of the fault. Offset ridges and gullies are clearly evident, as is the hillside bench cut by the main fault trace. Thin contour lines are at 25-cm and thick contour lines are at 2-m intervals. The area shown is an expanded view of features shown in Figure 4, here measuring 80 m (east–west) by 100 m (north–south).

Discussion

These laser data densely sampled the ground surface, and as such lend themselves to quantitatively estimating fault-slip vectors along the fault. Furthermore, because such data are systematically collected along the entire fault, we expect that a timely airborne survey after a future surface-rupturing event will make it possible to determine a continuous distribution of surface slip along the fault. Methods initially developed to quantify slip at a locality will be applied along the rest of the fault, after further testing and improvements.

As with other methods, however, laser scanning has its own unique capabilities and limitations, and we now discuss some of its relative merits in comparison with better-known methods. InSAR images tend to decorrelate close to the fault because of high strains and the effects of shaking disturbance to the ground surface. Decorrelation, while problematic with C-band InSAR, is expected to be much less so with L-band InSAR in the future. InSAR, moreover, can yield ground deformation in an absolute frame of reference, as can GPS and laser scanning. Field observations of surface offsets, on the other hand, tend to measure the slip vector by using features offset across discrete fault breaks, that is, relative rather than absolute displacement. Detailed topographic mapping using total-station instruments is time consuming, which proved difficult after the Hector Mine earthquake because geologists' field work was constrained by the USMC schedule.

Laser scanning of faults, especially when done both before and after future earthquakes, promises to be strongly complementary to surface-rupture mapping, InSAR, and GPS. It worked well in this case, in places, for several reasons. First, because the faults that ruptured in the Hector Mine earthquake had not ruptured for thousands of years, the pre-existing topography had low relief. It was therefore easy to uniquely discern the topographic features caused by slip in this earthquake from that associated with previous earthquakes. Second, it worked well in places with well-defined topographic features crossing the fault and with indurated materials on both sides of the fault. The Hector Mine surface rupture was like this along much of its length; earthquakes in other geologic settings may be less suitable for this approach. The method did not work well in flat-lying terrain with poorly consolidated, alluvial deposits. The laser-scanning method is becoming sufficiently precise that repeat-pass use should allow differential positioning at the centimeter level in both horizontal and vertical components (with some spatial averaging) to be obtained after future earthquakes, as long as pre-earthquake data are obtained with which to form a difference image. Laser scanning can be made to work in densely forested regions. The complementary use of digital photography with laser scanning, which worked well in our case, would of course be limited by trees.

During discussions on the EarthScope initiative and geological aspects of the Plate Boundary Observatory (*http://www.earthscope.org/PBOwhitepaper.pdf*), it has been proposed that systematic, topographic mapping of all active faults within the region of interest should be made in order to improve the currently available digital-elevation models. One possible method for obtaining such data is laser scanning, although radar and other methods will contribute as well. Our results show that laser scanning can be carried out effectively, in combination with other imaging, to a very high level of detail. To improve postearthquake damage assessment and disaster-recovery efforts, at the same time that strip mapping along active faults is performed, major lifelines that cross these faults should also be scanned.

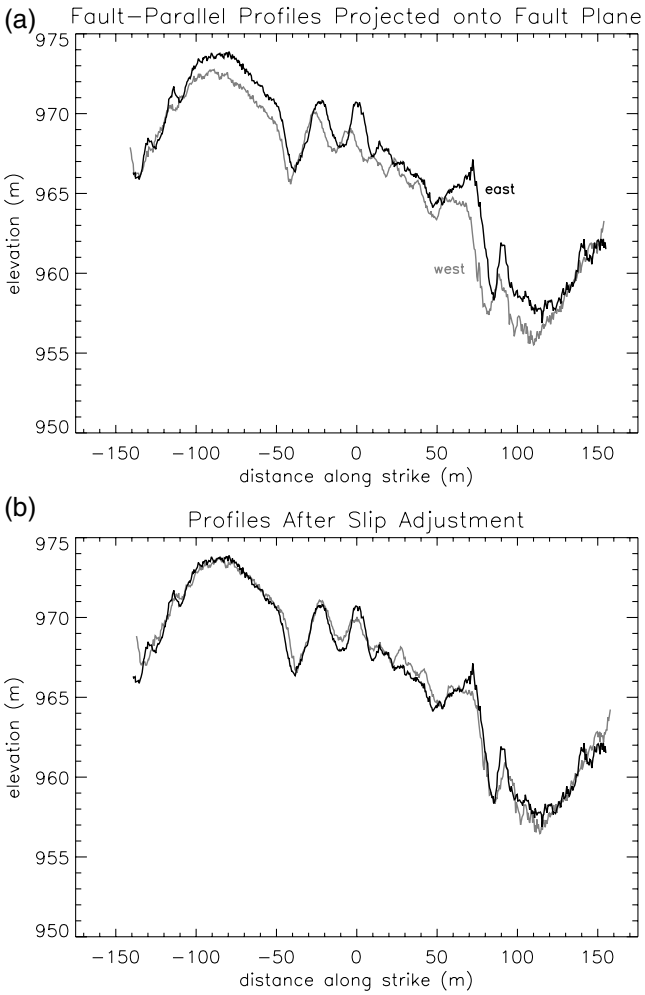

Figure 6. (a) Cross sections through the raw laser data on either side of the surface rupture, along the east and west profiles shown in Figure 4, are shown projected onto the fault plane (a ground-slope correction has already been removed). (b) Comparison of the topographic profiles on either side of the fault, after shifting the profiles shown in Figure 6a to remove our best estimate of the lateral and vertical offset along this 300-m section.

Acknowledgments

Without the permission and support of the U.S. Marine Corps Air Ground Combat Center in Twentynine Palms, California, we would not have been able to conduct this study. In particular, we thank Lt. Col. James J. Tabak for his support. Also, W. Karl Gross of the USGS, as liaison with the Marine Corps, provided invaluable assistance with field and aircraft logistics. Bill Krabill provided advice on methods and calibration experiments and has since collected additional data along these flight lines for use in future comparative analyses. We also appreciate the support of Analytical Photogrammetric Services for providing the digital photogrammetric map of the Rheox Hector Mine area, along with the raw data for the gridded elevation data that we used in evaluating the accuracy of this method. Rheox, Inc., allowed us access to their mine to conduct control surveys and carry out other GPS surveys for our calibrations. The SCIGN and its sponsors, the W. M. Keck Foundation, National Aeronautics and Space Administration, National Science Foundation (NSF), and USGS, provided support in the collection of high-sampling-rate GPS data from the nearby SCIGN stations. For these SCIGN data that we used in aircraft positioning, we especially thank John Galetzka, Aris Aspiotes, Keith Stark, and Shannon van Wyk, all at the USGS–SCIGN group in Pasadena. We are also grateful to Jim Dow and others from Aerotec, LLC, for ensuring the success of this project. Reviews by Katherine Kendrick, Greg Anderson, Mark Simons, and Michael Rymer improved this manuscript. This research was funded by the USGS, the Institute of Geophysics and Planetary Physics of the University of California, and the Southern California Earthquake Center (SCEC). SCEC is funded by NSF Cooperative Agreement EAR-8920136 and USGS Cooperative Agreements 14-08-0001-A0899 and 1434-HQ-97AG01718. The SCEC contribution number for this article is 637.

References

Borsa, A., J.-B. Minster, and K. Hudnut (2001). Estimating fault displacement from the 1999 Hector Mine earthquake using LIDAR, *EOS* **82,** no. 47 F270.

Burnman, H. (2000). *Calibration and Orientation of Airborne Image and Laser Scanner Data Using GPS and INS,* Royal Institute of Technology, Stockholm.

Carter, W. E., and R. L. Shrestha (1997). Airborne laser swath mapping: instant snapshots of our changing beaches, In *Proceedings of the Fourth International Conference: Remote Sensing for Marine and Coastal Environments,* Environmental Research Institute of Michigan, Ann Arbor, **I,** 298–307.

Hector Mine Geologic Working Group (2002). Surface rupture, slip distribution and other geologic observations associated with the M 7.1 Hector Mine earthquake of 16 October 1999, *U.S. Geol. Surv. Open-File Rept.* (in prep.).

Hudnut, K. W., N. E. King, J. E. Galetzka, K. F. Stark, J. A. Behr, A. Aspiotes, S. van Wyk, R. Moffitt, S. Dockter, and F. Wyatt (2002). Continuous GPS observations of postseismic deformation following the 16 October 1999 Hector Mine, California, earthquake (M_w 7.1), *Bull. Seism. Soc. Am.* **92,** 1403–1422 (this issue).

Krabill, W. B., R. H. Thomas, C. F. Martin, R. N. Swift, and E. B. Frederick (1995). Accuracy of airborne laser altimetry over the Greenland ice sheet, *Int. J. Remote Sensing,* **16,** no. 7, 1211–1222.

Kurushin, R. A., A. Bayasgalan, M. Olziybat, B. Enhtuvshin, P. Molnar, C. Bayarsayhan, K. W. Hudnut, and J. Lin (1997). The surface rupture of the 1957 Gobi-Altay, Mongolia, earthquake, Geol. Soc. Am. Special Paper no. 320, 143 pp.

Lindvall, S., T. Rockwell, and K. Hudnut (1989). Evidence for prehistoric earthquakes on the Superstition Hills fault from offset geomorphic features, *Bull. Seism. Soc. Am.* **79,** no. 2, 342–361.

Ridgeway, J. R., J.-B. Minster, N. Williams, J. L. Bufton, and W. B. Krabill (1997). Airborne laser altimeter survey of Long Valley, California, *Geophys. J. Int.* **131,** no. 2, 267–280.

Rymer, M. J., G. G. Seitz, K. D. Weaver, A. Orgil, G. Faneros, J. C. Hamilton, and C. Goetz (2002). Geologic and paleoseismic study of the Lavic Lake fault at Lavic Lake playa, Mojave Desert, southern California, *Bull. Seism. Soc. Am.* **92,** 1577–1591 (this issue).

Sandwell, D. T., L. Sichoix, and B. Smith (2002). The 1999 Hector Mine earthquake, southern California: vector near-field displacement from ERS InSAR, *Bull. Seism. Soc. Am.* **92,** 1341–1354 (this issue).

Scientists of the Southern California Earthquake Center, and the California Division of Mines and Geology (2000). Preliminary report on the 16 October 1999 *M* 7.1 Hector Mine, Calif., earthquake, *Seism. Res. Lett.* **71,** no. 1, 11–23.

Simons, M., Y. Fialko, and L. Rivera (2002). Coseismic deformation from the 1999 M_w 7.1 Hector Mine, California, earthquake as inferred from GPS and InSAR observations, *Bull. Seism. Soc. Am.* **92,** 1390–1402 (this issue).

Treiman, J. A., K. J. Kendrick, W. A. Bryant, T. K. Rockwell, and S. F. McGill (2002). Primary surface rupture associated with the M_w 7.1 16 October 1999 Hector Mine earthquake, San Bernardino County, California, *Bull. Seism. Soc. Am.* **92,** 1171–1191 (this issue).

U. S. Geological Survey
525 S. Wilson Ave.
Pasadena, CA 91106
(K.W.H.)

Scripps Institution of Oceanography
Institute of Geophysics and Planetary Physics
University of California, San Diego
La Jolla, CA 92093
(A.B., J.-B.M.)

Aerotec, LLC
Bessemer, AL 35022
(C.G.)

Manuscript received 5 March 2002.